C. R. Physique 17 (2016) 934–945

Contents lists available at ScienceDirect

Comptes Rendus Physique

www.sciencedirect.com

Polariton physics / Physique des polaritons

Exciton-polaritons in lattices: A non-linear photonic simulator

Les polaritons excitoniques sur réseau : un simulateur photonique non linéaire

Alberto Amo [a], Jacqueline Bloch [a,b]

[a] *Centre de nanosciences et de nanotechnologies, CNRS, Université Paris-Sud, Université Paris-Saclay, C2N – Marcoussis, 91460 Marcoussis, France*
[b] *Physics Department, École polytechnique, 91128 Palaiseau cedex, France*

ARTICLE INFO

Article history:
Available online 25 August 2016

Keywords:
Polaritons
Nonlinear optics
Josephson effect
Flatband
Condensation
Honeycomb
Topology
Analog quantum simulation

ABSTRACT

Microcavity polaritons are mixed light–matter quasiparticles with extraordinary nonlinear properties, which can be easily accessed in photoluminescence experiments. Thanks to the possibility of designing the potential landscape of polaritons, this system provides a versatile photonic platform to emulate 1D and 2D Hamiltonians. Polaritons allow transposing to the photonic world some of the properties of electrons in solid-state systems, and to engineer Hamiltonians for photons with novel transport properties. Here we review some experimental implementations of polariton Hamiltonians using lattice geometries.

RÉSUMÉ

Les polaritons de cavités sont des quasi-particules hybrides lumière–matière. Ils présentent des propriétés non linéaires extraordinaires, que l'on peut observer aisément dans des expériences de photoluminescence. En sculptant la forme du potentiel ressenti par les polaritons, on obtient une plateforme photonique particulièrement versatile pour émuler des hamiltoniens 1D ou 2D. Ainsi, les polaritons nous permettent-ils de transposer dans le monde photonique certaines des propriétés des électrons dans les solides et de donner à des photons de nouvelles propriétés de transport. Dans cet article, nous présentons quelques-unes des implémentations expérimentales des hamiltoniens pour les polaritons, qui sont basées sur différentes géométries de réseaux.

E-mail address: alberto.amo@lpn.cnrs.fr (A. Amo).

http://dx.doi.org/10.1016/j.crhy.2016.08.007

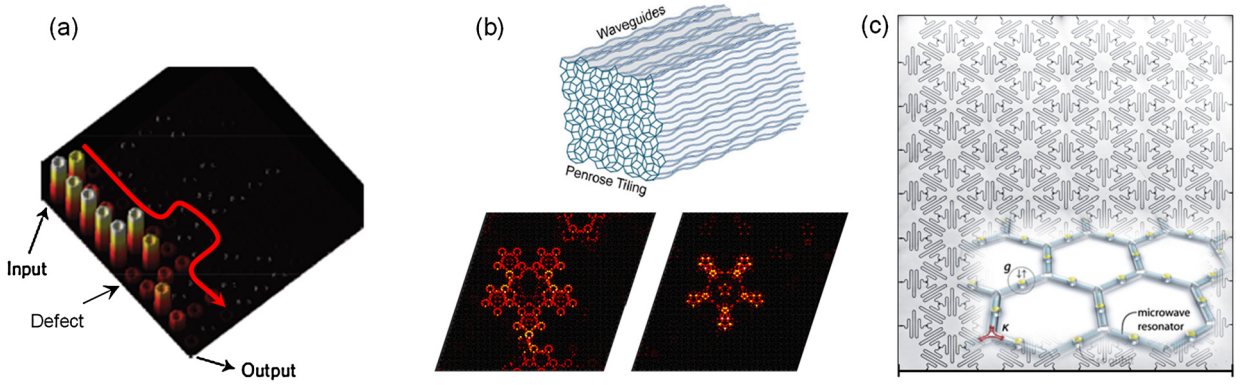

Fig. 1. (a) Photonic lattice made out of evanescently coupled Si resonator waveguides, which implements an artificial gauge field. Light tunnels from waveguide to waveguide along the edge of the lattice in a given direction. When a defect is encountered, photons go around it without backscattering. From Ref. [7]. (b) Scheme of the proposal to use coupled waveguides to realise a 2D quasicrystal with topological properties. Some of the bulk eigenstates of the crystal are shown in the lower panels. From Ref. [14]. (c) Kagome lattice of microwave resonators simulating the physics of graphene. From Ref. [32].

1. Introduction

Photonic simulators have appeared in the past few years as powerful platforms for experimental studies of elaborate Hamiltonians. The use of photons allows a simple initialisation of the wavefunction in the simulator, while observables like the amplitude, the phase, or the coherence properties of the wavepackets evolving in the simulator can be directly accessed using standard optical techniques. The ability to produce on-demand a number of quantum states of light, like squeezed and entangled states or indistinguishable photons, has put photonic simulators at the forefront of quantum physics, allowing, for example, the study of the boson sampling problem [1–3] and the quantum walk with indistinguishable particles [4]. At the classical level, photonic simulators have played a key role in the implementation of artificial gauge fields for neutral particles, and have allowed the experimental investigation of Anderson localisation [5], topological insulators [6,7], quantum spin- [8,9] and the anomalous Hall effect [10], Floquet Hamiltonians [11], topological classes in aperiodic systems [12–14], and the direct measurement of Chern numbers in photonic bands [15].

The archetypical ingredients of a photonic simulator are: (i) an array of sites in which photons are trapped or can travel in a confined way (i.e. optical cavities or waveguides), and (ii) a controlled hopping amplitude between sites. Additional properties like nonlinearities or onsite gain and losses can be added to extend the classes of accessible Hamiltonians. Ranging from micron size in the near-infrared to millimetres in the case of microwaves, the large wavelength of the photons employed in these simulators allows fabricating photonic lattices with a high degree of precision using standard lithographic and 3D laser imprinting techniques. Celebrated examples of simulators include lattices of microwave cavities [16–18], coupled optical parametric oscillators [19] and microlasers [20], and arrays of coupled waveguides arranged both in one and two dimensions [21]. The latter system has shown an extraordinary versatility in exploring solid-state Hamiltonians. The propagation of photons in arrays of coupled waveguides can be described in the paraxial approximation by a wave equation that is formally analogous to a conservative Schrödinger equation, in which the propagation distance plays the role of time. The evanescent tail of the electromagnetic field leaking out of the waveguides allows the engineering of the hopping between sites. Remarkable observations using these lattices include Bloch oscillations [22,23], dynamic localisation [24], modulation assisted tunnelling [25], Anderson localisation [5], transport in quasi-crystals [12,26], edge states in honeycomb lattices [27,28] or the implementation of artificial gauge fields [11,29]. By using nonlinear crystals and waveguides, soliton formation in discrete landscapes has been studied [30,31]. Fig. 1 shows different examples of photonic simulators using coupled waveguides.

A different system to implement photonic simulators is the semiconductor microcavity. Its eigenstates are cavity polaritons, exciton–photon mixed quasiparticles arising from the strong coupling between quantum-well excitons and cavity-confined photons. Thanks to the photonic component, polaritons possess an effective mass that is 10^{-5} times the mass of free electrons, and their amplitude, coherence and phase properties can be directly accessed from the leakage of photons through the Bragg mirrors that define the cavity [33]. The photonic part additionally allows the engineering of the polariton potential by laterally modifying the confinement of the cavity, as we shall see below.

2. Polariton interactions

One of the major assets of polaritons with respect to other confined optical systems is their extraordinary nonlinear properties, which arise from their excitonic component. They can be studied in two different types of configurations.

The first type is the so-called resonant excitation scheme, in which the energy and angle of incidence of the excitation laser are set to be quasi-resonant with a mode of the lower polariton branch. In this case, the dynamics of the polariton gas can be described by a driven-dissipative nonlinear Schrödinger equation:

$$i\hbar\frac{\partial\psi(r)}{\partial t}=\left[-\frac{\hbar^2\nabla^2}{2m^*}+V_{\text{ext}}(r)+g_{\text{p}}\left|\psi(r)\right|^2-i\frac{\hbar}{2}\gamma_{\text{p}}\right]\psi(r)+F(r,t)e^{-i(\omega t+kr)} \tag{1}$$

where $\psi(r)$ is the polariton wavefunction, m^* is the polariton effective mass, $V_{\text{ext}}(r)$ is the external potential, g_{p} is the polariton–polariton interaction constant (dependent on the exciton–photon detuning), γ_{p} is the polariton decay rate, and $F(r,t)$ is the amplitude of the pump laser with frequency ω and in-plane momentum k. Under intense pumping, polariton–polariton interactions dominate over kinetic energy, resulting in phenomena like optical parametric oscillation [34,35], squeezing [36,37], bistability [38], multistability [39,40], superfluidity [41], hydrodynamic vortices [42,43], and dark and bright solitons [44–46].

The second type of excitation is the so-called non-resonant one, in which the excitation laser has energy much higher than the lower polariton branch. In this case, polaritons can spontaneously form macroscopic coherent states, i.e. polariton lasers, by accumulation of particles in the same state [47]. At the condensation threshold, polaritons show a strongly non-linear input–output behaviour characteristic of bosonic stimulation, and the steady state is set by the interplay of pump, relaxation, and decay [47–49]. Their excitonic component results in significant interparticle interactions. They can be of two types: (i) polariton–polariton interactions in the macroscopically occupied state; (ii) interactions between polaritons and uncondensed excitons that accumulate in a reservoir at high energies.

A description of the polariton dynamics in the condensed regime under non-resonant excitation can be done in terms of a nonlinear Schrödinger equation with pump and losses [50]:

$$i\hbar\frac{\partial\psi(r)}{\partial t}=\left[-\frac{\hbar^2\nabla^2}{2m^*}+V_{\text{ext}}(r)+g_{\text{p}}\left|\psi(r)\right|^2+g_{\text{R}}n_{\text{R}}(r)+i\frac{\hbar}{2}\left[R\cdot n_{\text{R}}(r)-\gamma_{\text{p}}\right]\right]\psi(r) \tag{2}$$

Here g_{R} is the polariton–exciton interaction constant, $n_{\text{R}}(r)$ is the density of uncondensed reservoir excitons, and R is the relaxation rate of excitons into the condensed mode. This equation is coupled with the reservoir dynamics, which is fed by the excitation laser:

$$\frac{\partial n_{\text{R}}(r)}{\partial t}=-\frac{n_{\text{R}}(r)}{\tau_{\text{R}}}-R\cdot n_{\text{R}}(r)\left|\psi(\boldsymbol{r},t)\right|^2+P(r) \tag{3}$$

where τ_{R} is the nonradiative recombination of excitons and $P(r)$ is the laser pump intensity.

The interactions between polaritons and reservoir excitons have been used to optically engineer the polariton landscape. This can be done by injecting reservoir excitons in specific areas of the sample. As excitons have a much heavier mass than polaritons, they spread very little (on the micron scale) from the point where they are excited; thus, by using a proper combination of non-resonant excitation beams, the potential landscape seen by polaritons can be modified by the injection of excitons. This technique has been used to accelerate [51–53], stop [54], trap polaritons [55,56] and set them in rotation [57].

3. Polariton confinement

The confinement of polaritons can be engineered by tailoring the term $V_{\text{ext}}(r)$ in Eqs. (1) and (2). Several techniques have been used to reduce the dimensionality of polaritons. They include strain-induced traps [58], the use of hybrid air gap microcavities [59–61], surface acoustic waves [62], modification of the optical potential by gold deposition [63] or during-growth etching of the cavity layer [64,65] [the latter two are illustrated in Fig. 2a–b].

One of the most flexible techniques to tailor the polariton landscape is the post-growth deep lateral etching of the microcavity [Fig. 2c]: the strong refractive index contrast between the semiconductor and the air confines laterally the photonic component of polaritons inside the microstructure [66]. This technique has permitted the fabrication of 1D polariton circuits [51,67,68], interferometers [69] and diodes [70,71]. In this paper, we will review some of the properties of the first polariton lattices fabricated using this technique.

4. Coupled micropillars

The flexibility of semiconductor microcavities to engineer artificial Hamiltonians takes its full span when considering the coupling of micropillars. In an individual micropillar, polaritons are confined in the three directions in space, resulting in a discrete (gapped) spectrum [74]. The lowest energy mode presents a cylindrical, Gaussian-like amplitude distribution. The individual micropillars constitute the first ingredient to fabricate a polariton simulator, playing the role of a single site. The second ingredient is the controlled hopping between two different sites. This can be achieved by spatially overlapping two micropillars, as shown in Fig. 3a. The constriction between the pillars results in a photonic potential barrier through which the photonic component of the confined polaritons can tunnel. The height of the barrier depends on the overlap between the micropillars, thus allowing the engineering of the hopping amplitude (Fig. 3(b)) [75]. The system can be well described

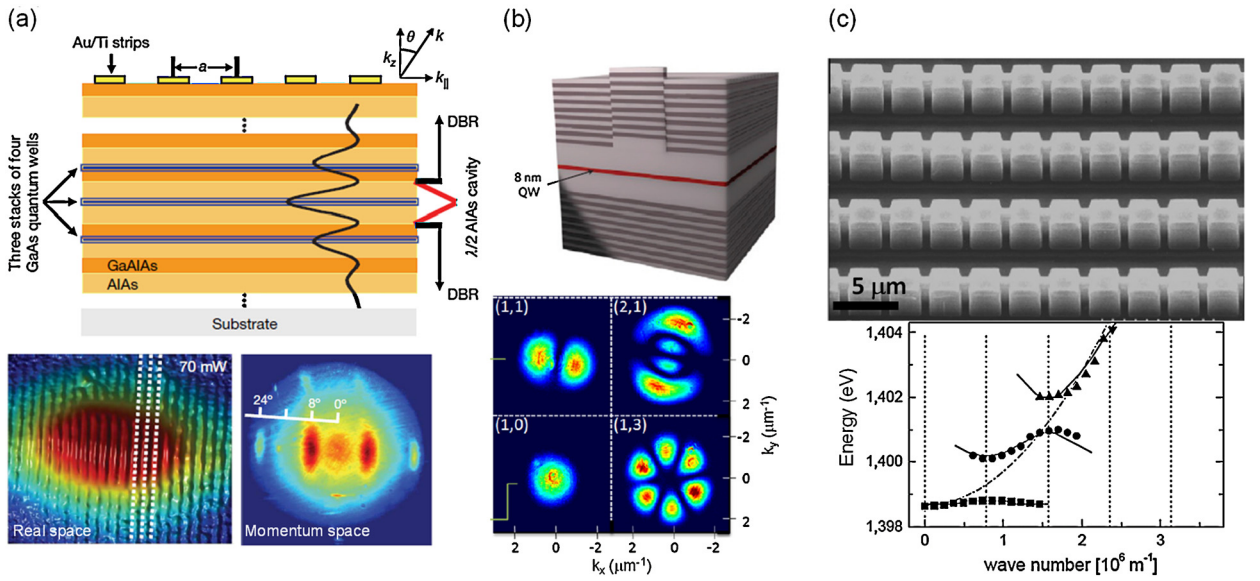

Fig. 2. (a) 1D lattice made by deposition of gold stripes in a planar microcavity. The bottom panels show the emission in real- (left) and momentum-space (right) of a polariton condensate formed in this structure. From Ref. [63]. (b) Scheme of a microcavity with a "mesa" fabricated by etching during the growth, and some of its confined polariton wavefunctions. From Refs. [39,72]. (c) A series of 1D periodic etched photonic lattices showing minibands and minigaps. From Ref. [73].

by a tight-binding Hamiltonian [76], in which onsite interaction, pump and losses characteristic of the polaritons can be included to model the steady-state emission of the system [33].

Already when considering just a small number of coupled micropillars, polariton nonlinearities give rise to interesting phenomena. For instance, the coupling of two micropillars allows addressing the physics of the nonlinear bosonic Josephson junction, whose dynamics are intimately related to the Josephson effect in superconductors [77]. The bosonic Josephson junction was introduced in the context of atomic Bose–Einstein condensates and presents different regimes depending on the interplay of onsite energy, hopping, and nonlinearity [78]. Resonant pulsed excitation allows preparing any at-will linear combination of the bonding and antibonding modes. Fig. 4 shows the evolution of a polariton wavepacket initialised by resonant pulsed excitation of one of the two coupled micropillars (labelled R in the figure) in three different regimes [79]. At low power [Fig. 4(a)], Rabi oscillations between the right and left micropillars are observed, with a period of about 21 ps. In this case, the energy of the ground state of each individual micropillar is equal, and the oscillation frequency is set by the tunnel coupling J (the period of oscillations is given by $T = h/2J$).

By injecting reservoir polaritons with a non-resonant laser in one of the micropillars, the local polariton energy can be modified via the term $g_R n_R(r)$ in Eq. (2). This is the case depicted in Fig. 4b, in which the oscillation period is now decreased to $T = h/\sqrt{4J^2 + (E^0_L - E^0_R)^2}$, where $E^0_{L(R)}$ is the energy of the ground state of the uncoupled left, L (right, R) micropillar. This situation corresponds to the so-called a.c. Josephson effect, and it was first demonstrated in polaritons by Lagoudakis and co-workers, making use of two disorder traps in a planar microcavity [80].

Finally, a strongly nonlinear regime can be achieved by resonantly injecting a large population of polaritons in one of the micropillars. This is the case depicted in Fig. 4c. Here the interaction energy in the right pillar $g_p|\psi_R(r)|^2$, is much larger than the tunnel coupling J. Therefore, the exchange of particles between the two micropillars is inhibited, and the system stays in a self-trapped regime for the first 60 ps. After that time, the escape of polaritons out of the cavity reduces the interaction energy and the system starts to oscillate.

The key element in the Josephson physics studied above is the combination of nonlinearity and the coupling between several modes. In the case of cw excitation, the same configuration gives rise to multistability [39,40] and self-pulsing [81]. More complex nonlinear effects are expected in photonic molecules with a larger number of sites [82,83]. If additionally the polarisation degree of freedom of polaritons is taken into account, it has been recently shown that a spin–orbit coupling Hamiltonian can be engineered using a hexagonal structure [84,85].

5. The 1D-Lieb lattice

When extending the coupling of micropillars to periodic structures, polariton energy bands can be engineered. The first polariton lattices were fabricated by the group of Y. Yamamoto [63] by depositing thin periodic gold stripes on top of a planar microcavity [see Fig. 2a]. The thin stripes locally alter the electromagnetic environment of the photonic mode reaching the surface of the cavity. However, the confinement thus achieved is relatively small compared to the polariton linewidth, and the engineered band gaps are hard to observe. A different technique was introduced by Cerda-Mendez and

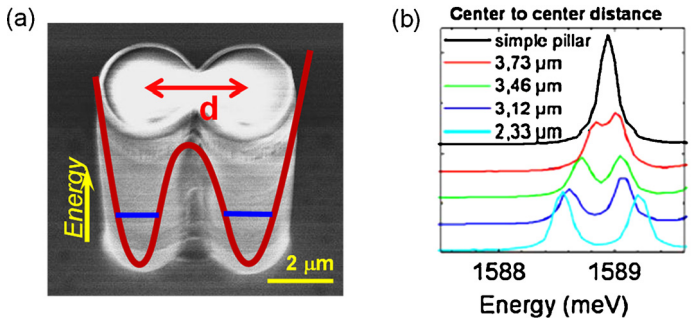

Fig. 3. (a) Scanning electron microscope image of two coupled micropillars. The centre-to-centre distance d is smaller than the diameter. Therefore, the micropillars overlap in space. (b) Spectrum of the lowest energy state of a single micropillar (black) with a diameter of 4 μm, and of two coupled micropillars with different centre-to-centre distances (indicated in the figure). The two peaks in the traces arise from the splitting between bonding and antibonding modes, whose magnitude is determined by the overlap. From Ref. [75].

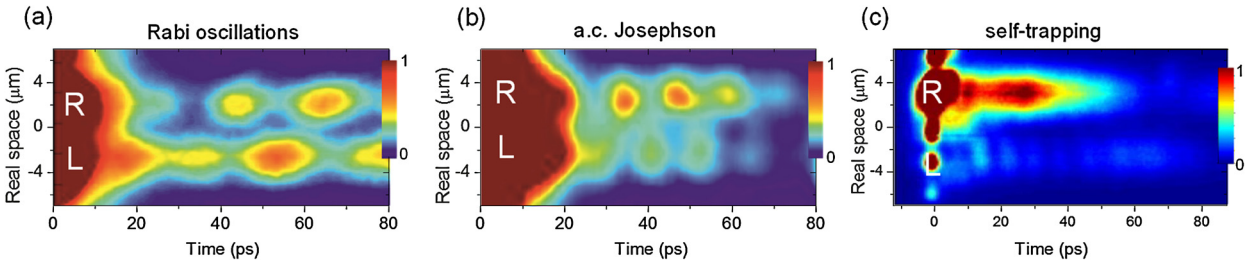

Fig. 4. Josephson oscillations in two coupled micropillars. (a) Linear Rabi regime with $E_L^0 = E_R^0$. (b) Linear a. c. Josephson regime with $E_L^0 \neq E_R^0$. (c) Nonlinear self trapping at high excitation density. From [79].

co-workers using surface acoustic waves, acting both on the excitonic and photonic components of polaritons [62]. While the potential depth of these lattices is higher than that of those fabricated using the gold deposition technique, this method is restricted to simple lattice geometries.

With respect to the aforementioned methods, the complete etching of micropillars provides a strong optical confinement, on-site control of the geometry and reduced polariton linewidth. It allows thus fabricating a wide variety of 1D and 2D lattices, including periodic [67] and aperiodic structures [68], and lattices with engineered disorder. An interesting example of lattices that can be engineered with this technique is a 1D lattice containing a flat energy band. This is the case of the so-called 1D-Lieb lattice (also known as Stub lattice) shown in Fig. 5a, made out of three sites per unit cell (A, B and C). The solution of the tight binding Hamiltonian for equal energies in sites A and C, independent of the absolute value of the nearest neighbour coupling, shows the formation of a flat energy band surrounded by two gapped dispersive bands, as reported experimentally in Fig. 5b. Note that in the flat band, the B pillars are dark. This arises from the destructive interference of the A and C photons, which in the flat band mode have opposite phases, when tunnelling to the B pillars.

Flat bands are particularly interesting because in the Hilbert sub-space of the eigenstates of the band, the Hamiltonian does not contain any kinetic energy term (the effective mass is infinite). Therefore, the physics of the system is dominated by any other term in the Hamiltonian, for instance, disorder or interactions [87–89]. As these terms act on the eigenstates in a non-perturbative way no matter their strength, it is not straightforward to compute the eigenenergies and eigenfunctions for large system sizes. The polariton simulator thus allows accessing this physics straightforwardly. Additionally, when the driven-dissipative nature of polaritons is taken into account, it allows addressing the question of the spatial and spectral shape of the lasing mode in a flat band [20]. Reviewing these phenomena, in particular the role of disorder, in polariton experiments will be the goal of this section. For further details, refer to Ref. [86] and works cited therein.

Fig. 6b–d shows the emission spectrum in momentum space for three different pumping powers. Only the emission linearly polarised along the long axis of the wire is selected. The structure is pumped non-resonantly with an elongated excitation spot centred on the geometrical centre of gravity of the structure, as sketched in Fig. 6a. At low pumping power (Fig. 6b), the three bands are homogeneously populated via incoherent relaxation. The dark areas at the centre of the first Brillouin zone appear as a consequence of the destructive interference characteristic of antibonding bands along high symmetry directions in momentum space [76].

Above a certain threshold pumping power P_{th} (Fig. 6d), polariton lasing takes place at the Γ point of the highest dispersive band. Lasing from this high energy state is not possible in systems in thermodynamic equilibrium, in which the state that accumulates the highest number of particles is the ground state and it is therefore the first to reach degeneracy. However, the polariton laser is out of equilibrium, its steady state is set by the interplay of pumping, relaxation and losses, and it can take place in excited states [90,91]. The lasing state is the first in which gain overcome losses when increasing the excitation power. A key parameter in setting the threshold is the overlap between a particular mode and the excitonic

reservoir that feeds it. As theoretically introduced by Ge et al. in Ref. [92], this overlap is strongly influenced both by polariton interactions, which modify the spatial shape of the polariton modes, and by the shape of the pumping spot. Taking advantage of these properties, polariton lasing in the flat band can be triggered by changing the pumping geometry such that the overlap between the pump laser and the flat band modes is enhanced. As the flat band modes have high probability amplitude in the external micropillars (Fig. 5c), shifting the pumping spot towards those pillars (Fig. 6g) allows lasing to happen in the flat band modes.

Fig. 6h–j shows the emission with the off-centred pumping configuration for polarisation perpendicular to the axis of the lattice. At low power (Fig. 6h), the bands are a bit different from the case of polarisation parallel to the lattice axis. The reason is the different confinement within the pillars for the two polarisations, which is strongly affected by the direction of the links to the adjacent pillars. For polarisation perpendicular to the lattice axis the photonic mode is more confined in pillars C than in pillars A. Therefore, the latter have a lower energy than the former. This breaks the condition for the existence of a flat band, and the three bands become dispersive, as shown in Fig. 6h.

When increasing the excitation density, the excitonic reservoir injected by the pumping laser interacts repulsively with the polariton modes: it induces a blueshift of the energy of the pumped micropillars. As the pumping spot is now centred on the external pillars, the blueshift is larger for the A than for the C pillars. Therefore, at intermediate powers the flat band condition (equal energy of A and C pillars) is restored for this polarisation, as shown in Fig. 6i. At even higher powers, lasing takes place in the flat band (Fig. 6j). In real space (Fig. 6k), the emission shows dark B pillars, characteristic of the flat band modes.

In the absence of any interaction or disorder, the flat band presents a high degeneracy (all flat band modes are at the same energy). The minimal size eigenmodes are plaquette states involving 1.5 unit cells [89,93]. By coherently adding plaquettes, any eigenmode size is possible from a single plaquette to an extended Bloch mode. An interesting question is then in which mode polariton lasing takes place.

A spectrum of the laser emission provides valuable information in this respect. Fig. 7b shows the energy and spatially resolved emission of the line of C pillars when lasing takes place in the flat band. Lasing in independent plaquettes of about 1–3 unit cells with different energies is observed. This is compatible with the smallest possible plaquette size in this lattice. In stark contrast, lasing from the upper dispersive band (Fig. 7a) shows a high spatial homogeneity in its spectral emission.

In the experiments reported in Fig. 7, very close to the threshold, polariton–polariton interactions within the condensate can be neglected. Fig. 7 thus shows the extreme sensitivity of the flat band modes to disorder. Both spectra have been measured on the exact same position of the 1D Lieb lattice. In the case of the polariton laser in the dispersive band, the effect of disorder is determined by the Anderson localisation physics. For the values of on-site disorder measured in our sample (about 30 μeV), the Anderson model predicts a localisation length of about 8 unit cells. For a strictly flat band, in the absence of dissipation (linewidth equal to zero), the expected localisation length is 1.5 plaquettes, independently of the disorder strength. This is the average size of the different energy plaquettes shown in Fig. 7b.

In the experiments discussed here, it has been evidenced the strong impact of disorder on the localisation of a polariton condensate in a flat band. Interesting avenues appear when these condensates are subject to high enough interactions. In this case, it has been predicted the formation of self-organised patterns at particular filling factors [89], and more recently, the emergence of quantum effects in the photon emission statistics [94]. Higher nonlinearities might be accessible via resonant injection of polaritons at the flat band energy, or by reducing the size of the micropillars and the number of quantum wells in the sample.

6. Two-dimensional lattices

More sophisticated band dispersions can be engineered by extending the lattices to two dimensions. The first works on 2D polariton lattices date back to 2011, with the report of polariton condensation in a square lattice fabricated using the gold deposition technique of the group of Yamamoto [95] (see Fig. 8a–c). This group has performed studies in triangular [96], hexagonal [97] and Kagome [98] lattices. However, the shallowness of the potential that can be implemented with this technique (on the order of the linewidth) has prevented the clear observation of the Dirac cones and two dimensional flat bands characteristic of the hexagonal and Kagome lattices, respectively. Deeper square lattices have been fabricated using either coupled mesas etched during the growth of the microcavity [65], or surface acoustic waves [99], allowing the observation of two-dimensional minibands and complete gaps (Fig. 8d–e). The lowest energy band of this square lattice presents a dispersion with an effective negative mass at the Brillouin zone edges. Using an optical parametric configuration, Cerda-Mendez and co-workers observed the nucleation of bright solitons in negative effective mass states [100]. Similar localised structures have been observed in 1D lattices with a periodic modulation [67].

The first two-dimensional polariton structure fabricated in fully etched microcavities was the honeycomb lattice (Fig. 9a) [76], which shares the same geometry as graphene. In this two-dimensional material, two of the three 2p orbitals of each carbon atom hybridize with the s orbitals to produce covalent bonds with three neighbouring carbon atoms, resulting in the honeycomb structure. The remaining p_z orbital of each carbon atom is cylindrically symmetric, sticks out of the atomic plane, and contains valence electrons that can tunnel from p_z orbital to p_z orbital. This hopping is well described by a tight binding Hamiltonian, and it gives rise to two dispersive bands that touch at six points in the first Brillouin zone – the so-called Dirac points [101].

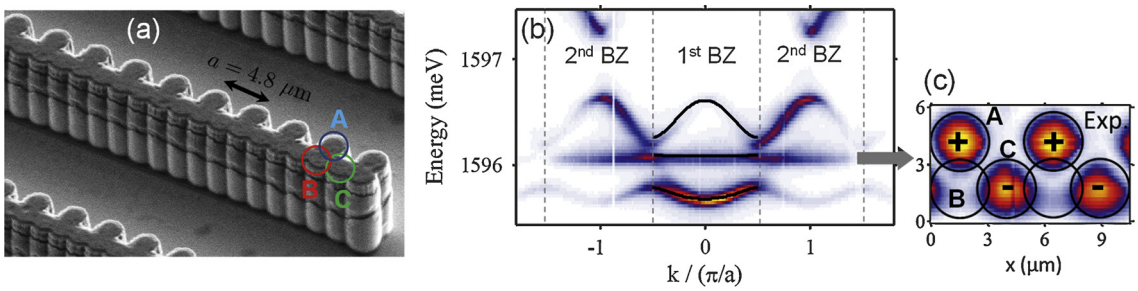

Fig. 5. (a) Scanning Electron Microscope image of a 1D Lieb lattice of coupled micropillars. (b) Measured polariton dispersion showing two dispersive bands above and below a flat band. The first, and second Brillouin zones (BZ) are shown. (c) Real space emission at the energy of the flat band, showing the spatial shape of the eigenmodes. From [86].

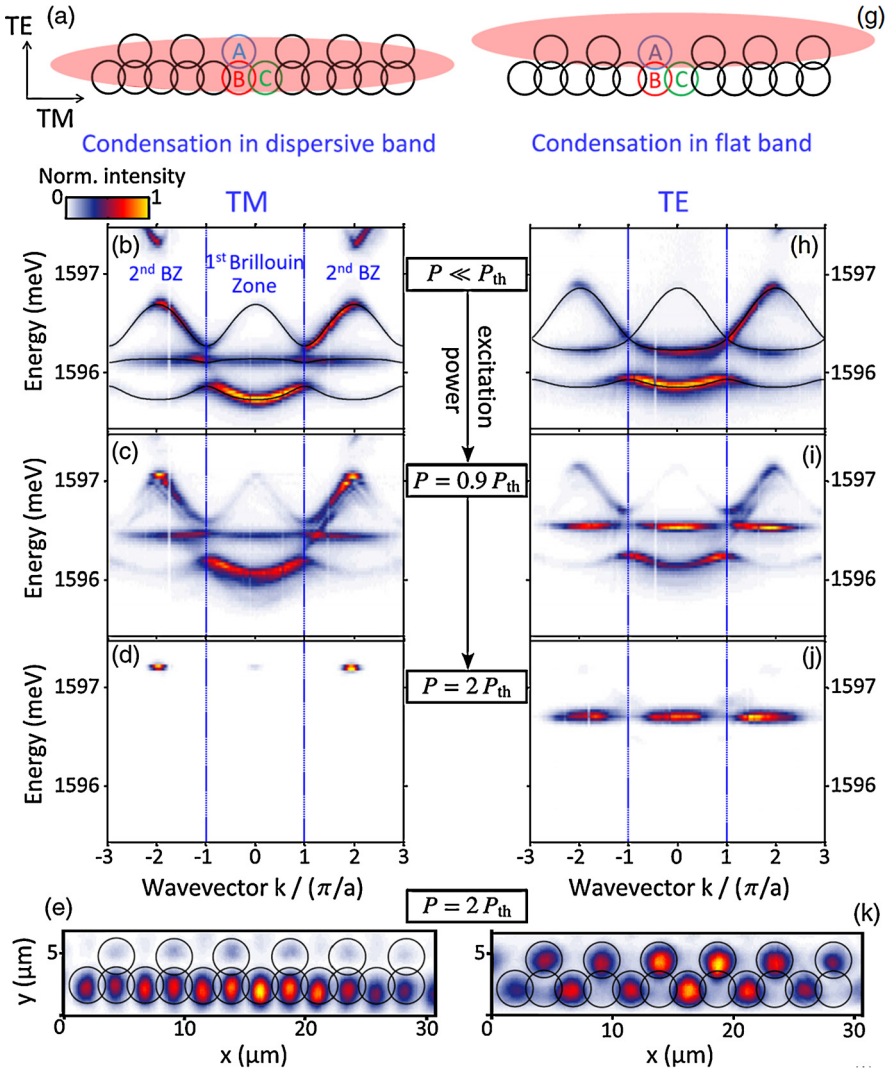

Fig. 6. (a) Symmetric pumping scheme allowing condensation in the dispersive band. (b)–(d) Spectra as a function of increasing excitation power for the pumping configuration shown in (a). The linear polarisation of the emission is selected in the direction parallel the lattice axis. (e) Measured spatial emission from the polariton laser formed at the top of the upper dispersive band at $2P_{th}$. (g) Pumping scheme enabling polariton lasing to take place in the flat band. (h)–(j) Spectra as a function of the excitation power for the pumping configuration shown in (g). The linear polarisation of the emission is selected in the direction perpendicular to the lattice axis. (k) Spatial emission from the polariton laser in the flat band (j). From Ref. [86].

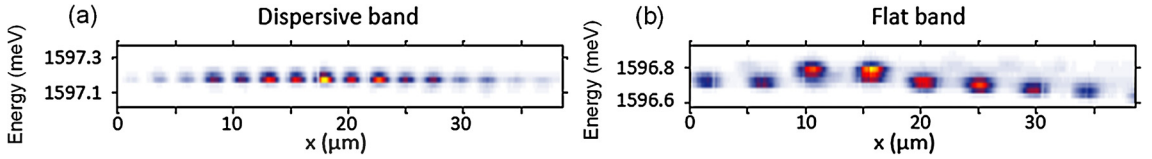

Fig. 7. Real space resolved spectrum of the polariton laser in the dispersive band (a) and in the flat band (b). From Ref. [86].

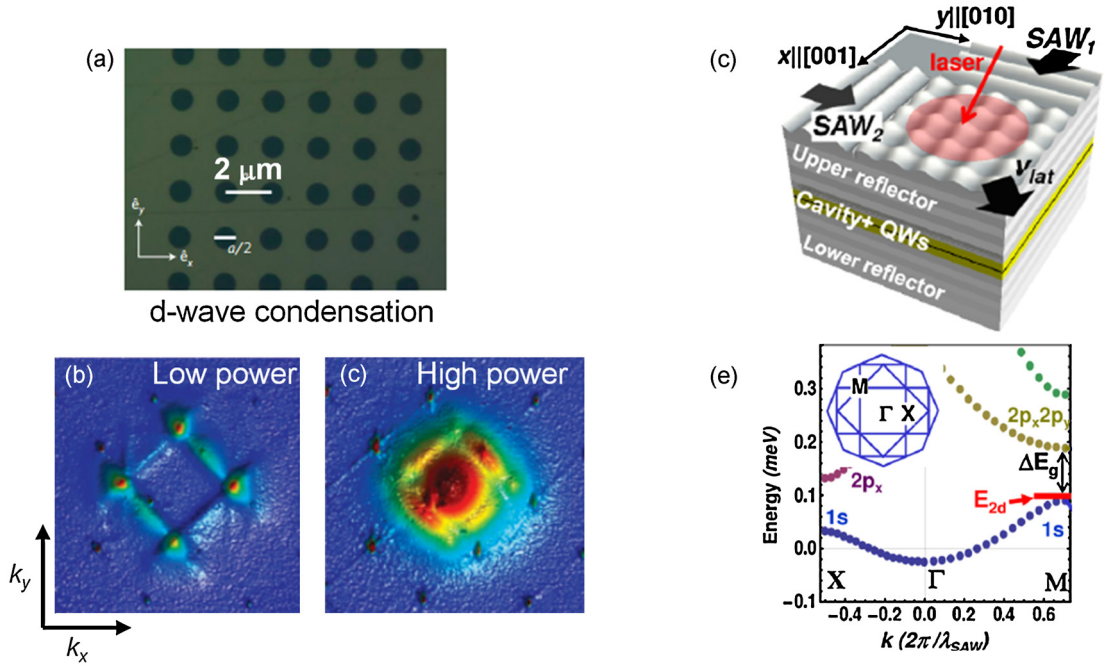

Fig. 8. (a) Polariton square lattice realised by gold deposition on the surface of the microcavity. (b–c) Momentum space emission at low (b) and high (c) power – above the condensation threshold. From Ref. [95]. (d) Scheme of the realisation of a square polariton lattice using surface acoustic waves (SAW). (e) Measured dispersion showing the opening of gaps and a negative effective mass at point M. From Ref. [100].

Fig. 9c shows the photoluminescence spectrum of a polariton honeycomb lattice. The characteristic linear dispersion around the six Dirac points is evidenced. This observation shows that we can transfer to the polariton system many of the well-known electronic properties of graphene. The direct access to the wavefunctions makes the polariton system particularly suitable for these studies. The eigenfunctions for energies close to the Dirac points present a spinor character with intriguing phase properties [101,102]. The conservation of the pseudospin results in the Klein tunnelling of electrons in graphene: the absence of backscattering when electrons encounter a potential barrier [103]. This phenomenon is related to weak antilocalisation in the presence of disorder, indirectly observed in electronic transport measurements [104], and accessible in a photonic system in the polariton honeycomb lattice.

Another consequence of the particular spinor structure of the wavefunction in a honeycomb lattice is the existence of edge states in finite size ribbons: it has been shown that the winding of the phase of the wavefunctions around the Dirac cones can be connected to the appearance of edge states similar to those emerging in the one-dimensional Su, Schrieffer, Heeger model [105]. The direct access to the wavefunction via the emitted photons permits the study of the edge states of this lattice. For instance, when exciting the lattice close to a zigzag edge, strong emission is observed from the last row of micropillars at the energy of the edge states expected from a calculation using a tight-binding Hamiltonian [106]. Similar edge states are also observed in the bearded edges, as expected and previously reported in coupled waveguide simulators [27].

A different striking effect accessible in this lattice is that of polariton lasing under out-of-resonance excitation [76]. Remarkably, lasing does not take place at the bottom of the lower polariton branch, but at the top of the band, as it was the case in the Lieb lattice. Polariton states at that point in the dispersion have an anti-bonding character with a zero of the wavefunction in the region between adjacent micropillars (see Fig. 9d), where losses are higher. The antibonding character of the lasing mode can be evidenced in an interferometric experiment as shown in Fig. 9e: the wavefunction presents a change in π between adjacent micropillars. The figure also shows the spatial coherence of the lasing mode, extended over several unit cells.

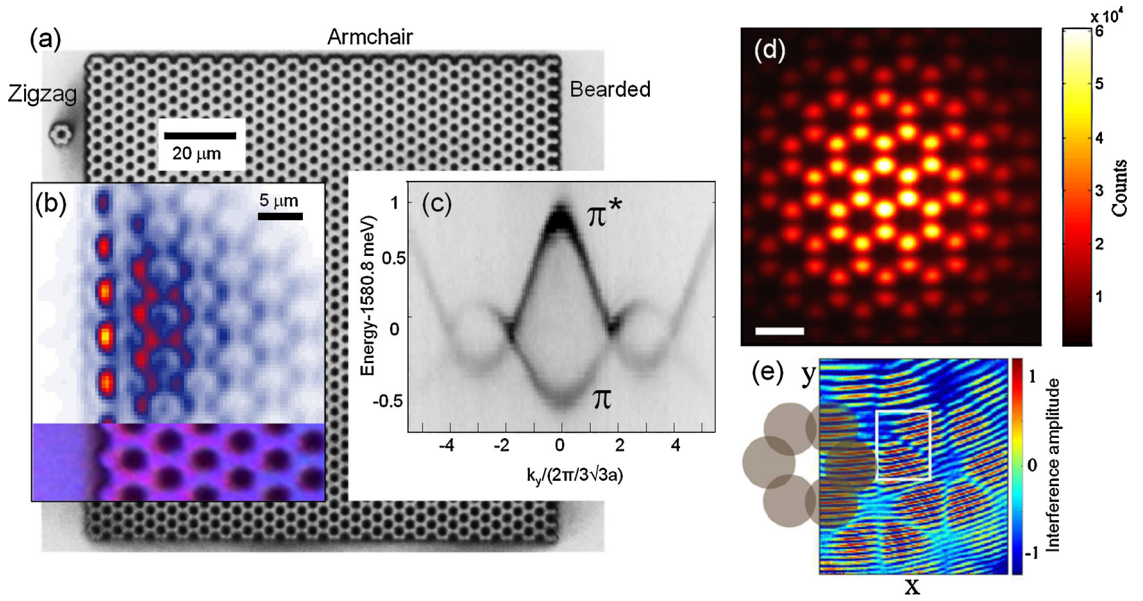

Fig. 9. (a) Optical microscope image of a polariton honeycomb lattice containing zigzag, armchair and bearded edges. (b) Photoluminescence at the energy of the zigzag edge states, showing enhanced emission on the left-most column of micropillars [106]. (c) Measured polariton dispersion of the honeycomb lattice showing the π and π^* bands [76]. (d) Polariton emission in the regime of polariton lasing. The emission originates from states at the top of the π^* band. (e) Interference pattern in the lasing regime made out of the combination of the real space emission from the lattice, with the enlarged emission from a single micropillar, which acts as a phase reference [76].

The polariton simulator provides a versatile sandpit to explore the influence of strain in the topological properties of hexagonal and other lattices. Merging of the Dirac cones [18,107,108], artificial gauge fields [29,109] and the appearance of novel edge states [28] can now be studied in a platform with unprecedented nonlinearities.

7. Perspectives

The combination of nonlinearities and lattices puts the polariton system at the forefront of research on quantum emulation in the solid state. Up to know, the nonlinear phenomena studied with microcavity polaritons have been restricted to the mean field level [33]. The possibility of reaching the quantum nonlinear regime, in which a single polariton would be enough to shift the onsite energy by more than the linewidth, would open new perspectives in the use of these quantum simulators. Expected phenomena are the single photon blockade [110], photon crystallisation [111,112], X–Y models [113] or the photonic analogue of the insulator–superfluid phase transition [114,115]. While this situation remains still a challenge, there have been interesting proposals and first experiments to increase the polariton nonlinearities, in particular by using the combination of polaritons with 2D electron gases [116].

Polariton lattices are also interesting in view of studying topological photonics. The intrinsic polarisation properties of polaritons [117] have been predicted to give rise to new types of spin–orbit coupling effects when combined with lattice geometries [118]. Additionally, either by using their nonlinear character [119,120], or their sensitivity to magnetic fields [121,122], polaritons in a lattice could give rise to chiral edge states with topologically protected transport.

Acknowledgements

We would like to acknowledge the members of the polariton group of the C2N Vera G. Sala, Félix Marsault, Marco Abbarchi, Thibaut Jacqmin, Marijana Milicevic, Said R. K. Rodriguez, Peristera Andreakou, Florent Baboux, Élisabeth Galopin, Aristide Lemaître, Isabelle Sagnes, and Luc Le Gratiet. This work was supported by the LABEX Nanosaclay project Qeage (Grant No. ANR-11-IDEX-0003-02), the ANR project Quandyde (ANR-11-BS10-001), the French RENATECH network, the ERC grant Honeypol and the EU-FET Proactiv grant AQUS (Project No. 640800).

References

[1] M.A. Broome, A. Fedrizzi, S. Rahimi-Keshari, J. Dove, S. Aaronson, T.C. Ralph, A.G. White, Photonic boson sampling in a tunable circuit, Science 339 (2013) 794–798.
[2] J.B. Spring, B.J. Metcalf, P.C. Humphreys, W.S. Kolthammer, X.-M. Jin, M. Barbieri, A. Datta, N. Thomas-Peter, N.K. Langford, D. Kundys, J.C. Gates, B.J. Smith, P.G.R. Smith, I.A. Walmsley, Boson sampling on a photonic chip, Science 339 (80) (2013) 798–801.
[3] M. Tillmann, B. Dakić, R. Heilmann, S. Nolte, A. Szameit, P. Walther, Experimental boson sampling, Nat. Photonics 7 (2013) 540–544.

[4] T. Kitagawa, M.A. Broome, A. Fedrizzi, M.S. Rudner, E. Berg, I. Kassal, A. Aspuru-Guzik, E. Demler, A.G. White, Observation of topologically protected bound states in photonic quantum walks, Nat. Commun. 3 (2012) 882.
[5] T. Schwartz, G. Bartal, S. Fishman, M. Segev, Transport and Anderson localization in disordered two-dimensional photonic lattices, Nature 446 (2007) 52–55.
[6] M. Hafezi, E.A. Demler, M.D. Lukin, J.M. Taylor, Robust optical delay lines with topological protection, Nat. Phys. 7 (2011) 907–912.
[7] M. Hafezi, S. Mittal, J. Fan, A. Migdall, J.M. Taylor, Imaging topological edge states in silicon photonics, Nat. Photonics 7 (2013) 1001–1005.
[8] F.D.M. Haldane, S. Raghu, Possible realization of directional optical waveguides in photonic crystals with broken time-reversal symmetry, Phys. Rev. Lett. 100 (2008) 13904.
[9] Z. Wang, Y. Chong, J.D. Joannopoulos, M. Soljacic, Observation of unidirectional backscattering-immune topological electromagnetic states, Nature 461 (2009) 772–775.
[10] T. Ozawa, I. Carusotto, Anomalous and quantum hall effects in lossy photonic lattices, Phys. Rev. Lett. 112 (2014) 133902.
[11] M.C. Rechtsman, J.M. Zeuner, Y. Plotnik, Y. Lumer, D. Podolsky, F. Dreisow, S. Nolte, M. Segev, A. Szameit, Photonic Floquet topological insulators, Nature 496 (2013) 196–200.
[12] Y.E. Kraus, Y. Lahini, Z. Ringel, M. Verbin, O. Zilberberg, Topological states and adiabatic pumping in quasicrystals, Phys. Rev. Lett. 109 (2012) 106402.
[13] M. Verbin, O. Zilberberg, Y.E. Kraus, Y. Lahini, Y. Silberberg, Observation of topological phase transitions in photonic quasicrystals, Phys. Rev. Lett. 110 (2013) 076403.
[14] M.A. Bandres, M.C. Rechtsman, M. Segev, Topological photonic quasicrystals: fractal topological spectrum and protected transport, Phys. Rev. X 6 (2016) 011016.
[15] S. Mittal, S. Ganeshan, J. Fan, A. Vaezi, M. Hafezi, Measurement of topological invariants in a 2D photonic system, Nat. Photonics 10 (2016) 180–183.
[16] S. Schmidt, D. Gerace, A.A. Houck, G. Blatter, H.E. Türeci, Nonequilibrium delocalization–localization transition of photons in circuit quantum electrodynamics, Phys. Rev. B 82 (2010) 100507(R).
[17] J. Raftery, D. Sadri, S. Schmidt, H.E. Türeci, A.A. Houck, Observation of a dissipation-induced classical to quantum transition, Phys. Rev. X 4 (2014) 031043.
[18] M. Bellec, U. Kuhl, G. Montambaux, F. Mortessagne, Topological transition of Dirac points in a microwave experiment, Phys. Rev. Lett. 110 (2013) 033902.
[19] A. Marandi, Z. Wang, K. Takata, R.L. Byer, Y. Yamamoto, Network of time-multiplexed optical parametric oscillators as a coherent Ising machine, Nat. Photonics 8 (2014) 937–942.
[20] M. Nixon, E. Ronen, A.A. Friesem, N. Davidson, Observing geometric frustration with thousands of coupled lasers, Phys. Rev. Lett. 110 (2013) 184102.
[21] D.N. Christodoulides, F. Lederer, Y. Silberberg, Discretizing light behaviour in linear and nonlinear waveguide lattices, Nature 424 (2003) 817–823.
[22] T. Pertsch, P. Dannberg, W. Elflein, A. Bräuer, F. Lederer, Optical Bloch oscillations in temperature tuned waveguide arrays, Phys. Rev. Lett. 83 (4752–4755) (1999).
[23] F. Dreisow, A. Szameit, M. Heinrich, T. Pertsch, S. Nolte, A. Tünnermann, S. Longhi, Bloch–Zener oscillations in binary superlattices, Phys. Rev. Lett. 102 (2009) 076802.
[24] S. Longhi, M. Marangoni, M. Lobino, R. Ramponi, P. Laporta, E. Cianci, V. Foglietti, Observation of dynamic localization in periodically curved waveguide arrays, Phys. Rev. Lett. 96 (2006) 243901.
[25] S. Mukherjee, A. Spracklen, D. Choudhury, N. Goldman, P. Öhberg, E. Andersson, R.R. Thomson, Modulation-assisted tunneling in laser-fabricated photonic Wannier–Stark ladders, New J. Phys. 17 (2015) 115002.
[26] L. Levi, M. Rechtsman, B. Freedman, T. Schwartz, O. Manela, M. Segev, Disorder-enhanced transport in photonic quasicrystals, Science 332 (2011) 1541–1544.
[27] Y. Plotnik, M.C. Rechtsman, D. Song, M. Heinrich, J.M. Zeuner, S. Nolte, Y. Lumer, N. Malkova, J. Xu, A. Szameit, Z. Chen, M. Segev, Observation of unconventional edge states in 'photonic graphene', Nat. Mater. 13 (2014) 57–62.
[28] M.C. Rechtsman, Y. Plotnik, J.M. Zeuner, D. Song, Z. Chen, A. Szameit, M. Segev, Topological creation and destruction of edge states in photonic graphene, Phys. Rev. Lett. 111 (2013) 103901.
[29] M.C. Rechtsman, J.M. Zeuner, A. Tunnermann, S. Nolte, M. Segev, A. Szameit, Strain-induced pseudomagnetic field and photonic Landau levels in dielectric structures, Nat. Photonics 7 (2013) 153–158.
[30] J.W. Fleischer, M. Segev, N.K. Efremidis, D.N. Christodoulides, Observation of two-dimensional discrete solitons in optically induced nonlinear photonic lattices, Nature 422 (2003) 147–150.
[31] O. Bahat-Treidel, O. Peleg, M. Segev, H. Buljan, Breakdown of Dirac dynamics in honeycomb lattices due to nonlinear interactions, Phys. Rev. A 82 (2010) 13830.
[32] A.A. Houck, H.E. Türeci, J. Koch, On-chip quantum simulation with superconducting circuits, Nat. Phys. 8 (2012) 292–299.
[33] I. Carusotto, C. Ciuti, Quantum fluids of light, Rev. Mod. Phys. 85 (2013) 299–366.
[34] M. Saba, C. Ciuti, J. Bloch, V. Thierry-Mieg, R. Andre Le Si Dang, S. Kundermann, A. Mura, G. Bongiovanni, J.L. Staehli, B. Deveaud, High-temperature ultrafast polariton parametric amplification in semiconductor microcavities, Nature 414 (2001) 731–735.
[35] P.G. Savvidis, J.J. Baumberg, R.M. Stevenson, M.S. Skolnick, D.M. Whittaker, J.S. Roberts, Angle-resonant stimulated polariton amplifier, Phys. Rev. Lett. 84 (2000) 1547.
[36] J.-P. Karr, A. Baas, R. Houdré, E. Giacobino, Squeezing in semiconductor microcavities in the strong-coupling regime, Phys. Rev. A 69 (2004) 31802.
[37] T. Boulier, M. Bamba, A. Amo, C. Adrados, A. Lemaitre, E. Galopin, I. Sagnes, J. Bloch, C. Ciuti, E. Giacobino, A. Bramati, Polariton-generated intensity squeezing in semiconductor micropillars, Nat. Commun. 5 (2014) 3260.
[38] A. Baas, J.Ph. Karr, H. Eleuch, E. Giacobino, Optical bistability in semiconductor microcavities, Phys. Rev. A 69 (2004) 23809.
[39] T.K. Paraïso, M. Wouters, Y. Leger, F. Mourier-Genoud, B. Deveaud-Pledran, Multistability of a coherent spin ensemble in a semiconductor microcavity, Nat. Mater. 10 (2011) 80.
[40] S.R.K. Rodriguez, A. Amo, I. Sagnes, L. Le Gratiet, E. Galopin, A. Lemaître, J. Bloch, Interaction-induced hopping phase in driven-dissipative coupled photonic microcavities, Nat. Commun. 7 (2016) 11887.
[41] A. Amo, J. Lefrère, S. Pigeon, C. Adrados, C. Ciuti, I. Carusotto, R. Houdré, E. Giacobino, A. Bramati, Superfluidity of polaritons in semiconductor microcavities, Nat. Phys. 5 (2009) 805–810.
[42] G. Nardin, G. Grosso, Y. Léger, B. Pietka, F. Morier-Genoud, B. Deveaud-Pledran, Hydrodynamic nucleation of quantized vortex pairs in a polariton quantum fluid, Nat. Phys. 7 (2011) 635–641.
[43] D. Sanvitto, S. Pigeon, A. Amo, D. Ballarini, M. De Giorgi, I. Carusotto, R. Hivet, F. Pisanello, V.G. Sala, P.S.S. Guimaraes, R. Houdré, E. Giacobino, C. Ciuti, A. Bramati, G. Gigli, All-optical control of the quantum flow of a polariton condensate, Nat. Photonics 5 (2011) 610–614.
[44] A. Amo, S. Pigeon, D. Sanvitto, V.G. Sala, R. Hivet, I. Carusotto, F. Pisanello, G. Leménager, R. Houdré, E. Giacobino, C. Ciuti, A. Bramati, Polariton superfluids reveal quantum hydrodynamic solitons, Science 332 (2011) 1167–1170.
[45] G. Grosso, G. Nardin, F. Morier-Genoud, Y. Léger, B. Deveaud-Plédran, Soliton instabilities and vortex street formation in a polariton quantum fluid, Phys. Rev. Lett. 107 (2011) 245301.
[46] M. Sich, D.N. Krizhanovskii, M.S. Skolnick, A.V. Gorbach, R. Hartley, D.V. Skryabin, E.A. Cerda-Mendez, K. Biermann, R. Hey, P.V. Santos, Observation of bright polariton solitons in a semiconductor microcavity, Nat. Photonics 6 (2012) 50–55.

[47] J. Kasprzak, M. Richard, S. Kundermann, A. Baas, P. Jeambrun, J.M.J. Keeling, F.M. Marchetti, M.H. Szymanska, R. Andre, J.L. Staehli, V. Savona, P.B. Littlewood, B. Deveaud, L.S. Dang, Bose–Einstein condensation of exciton polaritons, Nature 443 (2006) 409–414.
[48] G. Christmann, R. Butte, E. Feltin, J.F. Carlin, N. Grandjean, Room temperature polariton lasing in a GaN/AlGaN multiple quantum well microcavity, Appl. Phys. Lett. 93 (2008) 51102.
[49] S. Kena-Cohen, S.R. Forrest, Room-temperature polariton lasing in an organic single-crystal microcavity, Nat. Photonics 4 (2010) 371–375.
[50] M. Wouters, I. Carusotto, Excitations in a nonequilibrium Bose–Einstein condensate of exciton polaritons, Phys. Rev. Lett. 99 (2007) 140402.
[51] E. Wertz, L. Ferrier, D.D. Solnyshkov, R. Johne, D. Sanvitto, A. Lemaitre, I. Sagnes, R. Grousson, A.V. Kavokin, P. Senellart, G. Malpuech, J. Bloch, Spontaneous formation and optical manipulation of extended polariton condensates, Nat. Phys. 6 (2010) 860–864.
[52] E. Kammann, T.C.H. Liew, H. Ohadi, P. Cilibrizzi, P. Tsotsis, Z. Hatzopoulos, P.G. Savvidis, A.V. Kavokin, P.G. Lagoudakis, Nonlinear optical spin hall effect and long-range spin transport in polariton lasers, Phys. Rev. Lett. 109 (2012) 36404.
[53] B. Nelsen, G. Liu, M. Steger, D.W. Snoke, R. Balili, K. West, L. Pfeiffer, Dissipationless flow and sharp threshold of a polariton condensate with long lifetime, Phys. Rev. X 3 (2013) 041015.
[54] T. Gao, P.S. Eldridge, T.C.H. Liew, S.I. Tsintzos, G. Stavrinidis, G. Deligeorgis, Z. Hatzopoulos, P.G. Savvidis, Polariton condensate transistor switch, Phys. Rev. B 85 (2012) 235102.
[55] G. Tosi, G. Christmann, N.G. Berloff, P. Tsotsis, T. Gao, Z. Hatzopoulos, P.G. Savvidis, J.J. Baumberg, Sculpting oscillators with light within a nonlinear quantum fluid, Nat. Phys. 8 (2012) 190–194.
[56] A. Askitopoulos, H. Ohadi, A.V. Kavokin, Z. Hatzopoulos, P.G. Savvidis, P.G. Lagoudakis, Polariton condensation in an optically induced two-dimensional potential, Phys. Rev. B 88 (2013) 041308.
[57] R. Dall, M.D. Fraser, A.S. Desyatnikov, G. Li, S. Brodbeck, M. Kamp, C. Schneider, S. Höfling, E.A. Ostrovskaya, Creation of orbital angular momentum states with chiral polaritonic lenses, Phys. Rev. Lett. 113 (2014) 200404.
[58] R. Balili, V. Hartwell, D. Snoke, L. Pfeiffer, K. West, Bose–Einstein condensation of microcavity polaritons in a trap, Science 316 (80) (2007) 1007–1010.
[59] B. Zhang, Z. Wang, S. Brodbeck, C. Schneider, M. Kamp, S. Höfling, H. Deng, Zero-dimensional polariton laser in a subwavelength grating-based vertical microcavity, Light Sci. Appl. 3 (2014) e135.
[60] S. Dufferwiel, F. Fras, A. Trichet, P.M. Walker, F. Li, L. Giriunas, M.N. Makhonin, L.R. Wilson, J.M. Smith, E. Clarke, M.S. Skolnick, D.N. Krizhanovskii, Strong exciton–photon coupling in open semiconductor microcavities, Appl. Phys. Lett. 104 (2014) 192107.
[61] B. Besga, C. Vaneph, J. Reichel, J. Estève, A. Reinhard, J. Miguel-Sánchez, A. Imamoğlu, T. Volz, Polariton boxes in a tunable fiber cavity, Phys. Rev. Appl. 3 (2015) 014008.
[62] E.A. Cerda-Méndez, D.N. Krizhanovskii, M. Wouters, R. Bradley, K. Biermann, K. Guda, R. Hey, P.V. Santos, D. Sarkar, M.S. Skolnick, Polariton condensation in dynamic acoustic lattices, Phys. Rev. Lett. 105 (2010) 116402.
[63] C.W. Lai, N.Y. Kim, S. Utsunomiya, G. Roumpos, H. Deng, M.D. Fraser, T. Byrnes, P. Recher, N. Kumada, T. Fujisawa, Y. Yamamoto, Coherent zero-state and π-state in an exciton-polariton condensate array, Nature 450 (2007) 529.
[64] R. Idrissi Kaitouni, O. El Daïf, A. Baas, M. Richard, T. Paraïso, P. Lugan, T. Guillet, F. Morier-Genoud, J.D. Ganière, J.L. Staehli, V. Savona, B. Deveaud, Engineering the spatial confinement of exciton polaritons in semiconductors, Phys. Rev. B 74 (2006) 155311.
[65] K. Winkler, J. Fischer, A. Schade, M. Amthor, R. Dall, J. Geßler, M. Emmerling, E.A. Ostrovskaya, M. Kamp, C. Schneider, S. Höfling, A polariton condensate in a photonic crystal potential landscape, New J. Phys. 17 (2015) 023001.
[66] M. Bayer, T. Gutbrod, J.P. Reithmaier, A. Forchel, T.L. Reinecke, P.A. Knipp, A.A. Dremin, V.D. Kulakovskii, Optical modes in photonic molecules, Phys. Rev. Lett. 81 (1998) 2582–2585.
[67] D. Tanese, H. Flayac, D. Solnyshkov, A. Amo, A. Lemaître, E. Galopin, R. Braive, P. Senellart, I. Sagnes, G. Malpuech, J. Bloch, Polariton condensation in solitonic gap states in a one-dimensional periodic potential, Nat. Commun. 4 (2013) 1749.
[68] D. Tanese, E. Gurevich, F. Baboux, T. Jacqmin, A. Lemaître, E. Galopin, I. Sagnes, A. Amo, J. Bloch, E. Akkermans, Fractal energy spectrum of a polariton gas in a Fibonacci quasiperiodic potential, Phys. Rev. Lett. 112 (2014) 146404.
[69] C. Sturm, D. Tanese, H.S. Nguyen, H. Flayac, E. Galopin, A. Lemaître, I. Sagnes, D. Solnyshkov, A. Amo, G. Malpuech, J. Bloch, All-optical phase modulation in a cavity-polariton Mach–Zehnder interferometer, Nat. Commun. 5 (2014) 3278.
[70] H.S. Nguyen, D. Vishnevsky, C. Sturm, D. Tanese, D. Solnyshkov, E. Galopin, A. Lemaître, I. Sagnes, A. Amo, G. Malpuech, J. Bloch, Realization of a double-barrier resonant tunneling diode for cavity polaritons, Phys. Rev. Lett. 110 (2013) 236601.
[71] F. Marsault, H.S. Nguyen, D. Tanese, A. Lemaître, É. Galopin, I. Sagnes, A. Amo, J. Bloch, Realization of an all optical exciton-polariton router, Appl. Phys. Lett. 107 (2015) 201115.
[72] R. Cerna, D. Sarchi, T.K. Paraïso, G. Nardin, Y. Léger, M. Richard, B. Pietka, O. El Daif, F. Morier-Genoud, V. Savona, M.T. Portella-Oberli, B. Deveaud-Plédran, Coherent optical control of the wave function of zero-dimensional exciton polaritons, Phys. Rev. B 80 (2009) 121309.
[73] M. Bayer, T. Gutbrod, A. Forchel, T.L. Reinecke, P.A. Knipp, R. Werner, J.P. Reithmaier, Optical demonstration of a crystal band structure formation, Phys. Rev. Lett. 83 (1999) 5374–5377.
[74] D. Bajoni, P. Senellart, E. Wertz, I. Sagnes, A. Miard, A. Lemaître, J. Bloch, Polariton laser using single micropillar GaAs–GaAlAs semiconductor cavities, Phys. Rev. Lett. 100 (2008) 47401.
[75] M. Galbiati, L. Ferrier, D.D. Solnyshkov, D. Tanese, E. Wertz, A. Amo, M. Abbarchi, P. Senellart, I. Sagnes, A. Lemaitre, É. Galopin, G. Malpuech, J. Bloch, Polariton condensation in photonic molecules, Phys. Rev. Lett. 108 (2012) 126403.
[76] T. Jacqmin, I. Carusotto, I. Sagnes, M. Abbarchi, D. Solnyshkov, G. Malpuech, É. Galopin, A. Lemaître, J. Bloch, A. Amo, Direct observation of Dirac cones and a flatband in a honeycomb lattice for polaritons, Phys. Rev. Lett. 112 (2014) 116402.
[77] S. Levy, E. Lahoud, I. Shomroni, J. Steinhauer, The a.c. and d.c. Josephson effects in a Bose–Einstein condensate, Nature 449 (2007) 579–583.
[78] S. Raghavan, A. Smerzi, S. Fantoni, S.R. Shenoy, Coherent oscillations between two weakly coupled Bose–Einstein condensates: Josephson effects, π oscillations, and macroscopic quantum self-trapping, Phys. Rev. A 59 (1999) 620–633.
[79] M. Abbarchi, A. Amo, V.G. Sala, D.D. Solnyshkov, H. Flayac, L. Ferrier, I. Sagnes, E. Galopin, A. Lemaitre, G. Malpuech, J. Bloch, Macroscopic quantum self-trapping and Josephson oscillations of exciton polaritons, Nat. Phys. 9 (2013) 275–279.
[80] K.G. Lagoudakis, B. Pietka, M. Wouters, R. André, B. Deveaud-Plédran, Coherent oscillations in an exciton-polariton Josephson junction, Phys. Rev. Lett. 105 (2010) 120403.
[81] D. Sarchi, I. Carusotto, M. Wouters, V. Savona, Coherent dynamics and parametric instabilities of microcavity polaritons in double-well systems, Phys. Rev. B 77 (2008) 125324.
[82] E.A. Ostrovskaya, Y.S. Kivshar, Matter-wave gap vortices in optical lattices, Phys. Rev. Lett. 93 (2004) 160405.
[83] V.E. Lobanov, Y.V. Kartashov, V.A. Vysloukh, L. Torner, Stable radially symmetric and azimuthally modulated vortex solitons supported by localized gain, Opt. Lett. 36 (2011) 85–87.
[84] V.G. Sala, D.D. Solnyshkov, I. Carusotto, T. Jacqmin, A. Lemaître, H. Terças, A. Nalitov, M. Abbarchi, E. Galopin, I. Sagnes, J. Bloch, G. Malpuech, A. Amo, Spin–orbit coupling for photons and polaritons in microstructures, Phys. Rev. X 5 (2015) 011034.
[85] S. Dufferwiel, Feng Li, E. Cancellieri, L. Giriunas, A.A.P. Trichet, D.M. Whittaker, P.M. Walker, F. Fras, E. Clarke, J.M. Smith, M.S. Skolnick, D.N. Krizhanovskii, Spin textures of exciton-polaritons in a tunable microcavity with large TE-TM splitting, Phys. Rev. Lett. 115 (2015) 246401.
[86] F. Baboux, L. Ge, T. Jacqmin, M. Biondi, E. Galopin, A. Lemaître, L. Le Gratiet, I. Sagnes, S. Schmidt, H.E. Türeci, A. Amo, J. Bloch, Bosonic condensation and disorder-induced localization in a flat band, Phys. Rev. Lett. 116 (2016) 066402.

[87] C. Wu, D. Bergman, L. Balents, S. Das Sarma, Flat bands and Wigner crystallization in the honeycomb optical lattice, Phys. Rev. Lett. 99 (2007) 070401.
[88] S.D. Huber, E. Altman, Bose condensation in flat bands, Phys. Rev. B 82 (2010) 184502.
[89] M. Biondi, E.P.L. van Nieuwenburg, G. Blatter, S.D. Huber, S. Schmidt, Incompressible polaritons in a flat band, Phys. Rev. Lett. 115 (2015) 143601.
[90] M. Richard, J. Kasprzak, R. André, R. Romestain Le Si Dang, G. Malpuech, A. Kavokin, Experimental evidence for nonequilibrium Bose condensation of exciton polaritons, Phys. Rev. B 72 (2005) 201301(R).
[91] M. Wouters, I. Carusotto, C. Ciuti, Spatial and spectral shape of inhomogeneous nonequilibrium exciton-polariton condensates, Phys. Rev. B 77 (2008) 115340.
[92] L. Ge, A. Nersisyan, B. Oztop, H.E. Tureci, Pattern formation and strong nonlinear interactions in exciton-polariton condensates, arXiv: 1311.4847v1, 2013.
[93] R.A. Vicencio, C. Cantillano, L. Morales-Inostroza, B. Real, C. Mejía-Cortés, S. Weimann, A. Szameit, M.I. Molina, Observation of localized states in Lieb photonic lattices, Phys. Rev. Lett. 114 (2015) 245503.
[94] W. Casteels, R. Rota, F. Storme, C. Ciuti, Probing photon correlations in the dark sites of geometrically frustrated cavity lattices, Phys. Rev. A 93 (2015) 043833.
[95] N.Y. Kim, K. Kusudo, C. Wu, N. Masumoto, A. Loffler, S. Hofling, N. Kumada, L. Worschech, A. Forchel, Y. Yamamoto, Dynamical d-wave condensation of exciton-polaritons in a two-dimensional square-lattice potential, Nat. Phys. 7 (2011) 681–686.
[96] N.Y. Kim, K. Kusudo, A. Löffler, S. Höfling, A. Forchel, Y. Yamamoto, Exciton-polariton condensates near the Dirac point in a triangular lattice, New J. Phys. 15 (2013) 35032.
[97] K. Kusudo, N.Y. Kim, A. Löffler, S. Höfling, A. Forchel, Y. Yamamoto, Stochastic formation of polariton condensates in two degenerate orbital states, Phys. Rev. B 87 (2013) 214503.
[98] N. Masumoto, N.Y. Kim, T. Byrnes, K. Kusudo, A. Löffler, S. Höfling, A. Forchel, Y. Yamamoto, Exciton-polariton condensates with flat bands in a two-dimensional kagome lattice, New J. Phys. 14 (2012) 65002.
[99] E.A. Cerda-Méndez, D.N. Krizhanovskii, K. Biermann, R. Hey, M.S. Skolnick, P.V. Santos, Dynamic exciton-polariton macroscopic coherent phases in a tunable dot lattice, Phys. Rev. B 86 (2012) 100301.
[100] E.A. Cerda-Méndez, D. Sarkar, D.N. Krizhanovskii, S.S. Gavrilov, K. Biermann, M.S. Skolnick, P.V. Santos, Exciton-polariton gap solitons in two-dimensional lattices, Phys. Rev. Lett. 111 (2013) 146401.
[101] A.H. Castro Neto, F. Guinea, N.M.R. Peres, K.S. Novoselov, A.K. Geim, The electronic properties of graphene, Rev. Mod. Phys. 81 (2009) 109–162.
[102] D. Song, V. Paltoglou, S. Liu, Y. Zhu, D. Gallardo, L. Tang, J. Xu, M. Ablowitz, N.K. Efremidis, Z. Chen, Unveiling pseudospin and angular momentum in photonic graphene, Nat. Commun. 6 (2015) 6272.
[103] P. Allain, J.N. Fuchs, Klein tunneling in graphene: optics with massless electrons, EPJ B 83 (2011) 301–317.
[104] S.V. Morozov, K.S. Novoselov, M.I. Katsnelson, F. Schedin, L.A. Ponomarenko, D. Jiang, A.K. Geim, Strong suppression of weak localization in graphene, Phys. Rev. Lett. 97 (2006) 016801.
[105] P. Delplace, D. Ullmo, G. Montambaux, Zak phase and the existence of edge states in graphene, Phys. Rev. B 84 (2011) 195452.
[106] M. Milićević, T. Ozawa, P. Andreakou, I. Carusotto, T. Jacqmin, E. Galopin, A. Lemaître, L. Le Gratiet, I. Sagnes, J. Bloch, A. Amo, Edge states in polariton honeycomb lattices, 2D Mater. 2 (2015) 034012.
[107] G. Montambaux, F. Piéchon, J.N. Fuchs, M. Goerbig, Merging of Dirac points in a two-dimensional crystal, Phys. Rev. B 80 (2009) 153412.
[108] L. Tarruell, D. Greif, T. Uehlinger, G. Jotzu, T. Esslinger, Creating, moving and merging Dirac points with a Fermi gas in a tunable honeycomb lattice, Nature 483 (2012) 302–305.
[109] G. Salerno, T. Ozawa, H.M. Price, I. Carusotto, How to directly observe Landau levels in driven-dissipative strained honeycomb lattices, 2D Mater. 2 (2015) 034015.
[110] A. Verger, C. Ciuti, I. Carusotto, Polariton quantum blockade in a photonic dot, Phys. Rev. B 73 (2006) 193306.
[111] I. Carusotto, D. Gerace, H.E. Tureci, S. De Liberato, C. Ciuti, A. Imamoglu, Fermionized photons in an array of driven dissipative nonlinear cavities, Phys. Rev. Lett. 103 (2009) 33601.
[112] M.J. Hartmann, Polariton crystallization in driven arrays of lossy nonlinear resonators, Phys. Rev. Lett. 104 (2010) 113601.
[113] D.G. Angelakis, M. Franca Santos, S. Bose, Photon-blockade-induced Mott transitions and XY spin models in coupled cavity arrays, Phys. Rev. A 76 (2007) 31805.
[114] M.J. Hartmann, F.G.S.L. Brandao, M.B. Plenio, Strongly interacting polaritons in coupled arrays of cavities, Nat. Phys. 2 (2006) 849–855.
[115] A. Le Boité, G. Orso, C. Ciuti, Steady-state phases and tunneling-induced instabilities in the driven dissipative Bose–Hubbard model, Phys. Rev. Lett. 110 (2013) 233601.
[116] S. Smolka, W. Wuester, F. Haupt, S. Faelt, W. Wegscheider, A. Imamoglu, Cavity quantum electrodynamics with many-body states of a two-dimensional electron gas, Science 346 (2014) 332–335.
[117] A. Kavokin, G. Malpuech, M. Glazov, Optical spin Hall effect, Phys. Rev. Lett. 95 (2005) 136601.
[118] A.V. Nalitov, G. Malpuech, H. Terças, D.D. Solnyshkov, Spin–orbit coupling and the optical spin hall effect in photonic graphene, Phys. Rev. Lett. 114 (2015) 026803.
[119] C.-É. Bardyn, T. Karzig, G. Refael, T.C.H. Liew, Chiral Bogoliubov excitations in nonlinear bosonic systems, Phys. Rev. B 93 (2016) 020502.
[120] R.O. Umucalilar, I. Carusotto, Fractional quantum hall states of photons in an array of dissipative coupled cavities, Phys. Rev. Lett. 108 (2012) 206809.
[121] A.V. Nalitov, D.D. Solnyshkov, G. Malpuech, Polariton Z topological insulator, Phys. Rev. Lett. 114 (2015) 116401.
[122] T. Karzig, C.-É. Bardyn, N.H. Lindner, G. Refael, Topological polaritons, Phys. Rev. X 5 (2015) 031001.